4-1-2015

Molecular Mechanisms Of The Effect Of Ultrasound On The Fibrinolysis Of Clots

I. N. Chernysh

E. Carr Everbach
Swarthmore College, ceverba1@swarthmore.edu

P. K. Purohit

J. W. Weisel

HHS Public Access

Author manuscript

J Thromb Haemost. Author manuscript; available in PMC 2016 December 15.

Published in final edited form as:

J Thromb Haemost. 2015 April ; 13(4): 601–609. doi:10.1111/jth.12857.

Molecular mechanisms of the effect of ultrasound on the fibrinolysis of clots

Irina N. Chernysh[1], **E. Carr Everbach**[2], **Prashant K. Purohit**[3], and **John W. Weisel**[1,*]

[1]Department Cell and Developmental Biology, University of Pennsylvania School of Medicine, Philadelphia, PA 19104-6058, USA

[2]Engineering Department, Swarthmore College, Swarthmore, PA 19081-1397 USA

[3]Department of Mechanical Engineering and Applied Mechanics, University of Pennsylvania, Philadelphia, PA 19104-6315 USA

Summary

Background—Ultrasound accelerates tissue-type plasminogen activator (t-PA)-induced fibrinolysis of clots in vitro and in vivo.

Objective—To identify mechanisms for the enhancement of t-PA-induced fibrinolysis of clots.

Methods—Turbidity is an accurate and convenient method, not previously used, to follow the effects of ultrasound. Deconvolution microscopy was used to determine changes in structure, while fluorescence recovery after photobleaching was used to characterize the kinetics of binding/unbinding and transport.

Results—The ultrasound pulse repetition frequency affected clot lysis times, but there were no thermal effects. Ultrasound in the absence of t-PA produced a slight but consistent decrease in turbidity, suggesting a decrease in fibrin diameter due solely to the action of the ultrasound, likely caused by an increase in protofibril tension because of vibration from ultrasound. Changes in fibrin network structure during lysis with ultrasound were visualized in real time by deconvolution microscopy, revealing that the network becomes unstable when 30–40% of the protein in the network was digested, whereas without ultrasound, the fibrin network was digested gradually and retained structural integrity. Fluorescence recovery after photobleaching during lysis revealed that the off-rate of oligomers from digesting fibers was not much affected but the number of binding/unbinding sites was increased.

Conclusions—Ultrasound causes a decrease in the diameter of the fibers due to tension as a result of vibration, leading to increased binding sites for plasmin(ogen)/t-PA. The positive feedback of this structural change together with increased mixing/transport of t-PA/plasmin(ogen) is likely to account for the observed enhancement of fibrinolysis by ultrasound.

*To whom correspondence should be addressed: Department Cell and Developmental Biology, University of Pennsylvania School of Medicine, 421 Curie Blvd., 1154 BRB II/III, Philadelphia, PA 19104-6058, USA. Tel.: 215-898-3573, weisel@mail.med.upenn.edu.

Authorship

Contributions: I. N. Chernysh, E. C. Everbach, P. K. Purohit, and J. W. Weisel designed experiments and analyzed data. I. N. Chernysh performed experiments. The manuscript was written by I. N. Chernysh, E. C. Everbach, P. K. Purohit, and J. W. Weisel.

Authors state no conflicts of interests.

Keywords

fibrin; fibrinolysis; plasma; microscopy; ultrasound

Introduction

Fibrin polymerization also triggers the fibrinolytic system to dissolve the clot, with activation of plasminogen to plasmin by tissue plasminogen activator (t-PA) on the fibrin surface. However, fibrinolysis is not a simple proteolytic reaction, but a dynamic process involving activators and inhibitors. Fibrin plays a dual role in this process by enhancing the activity of t-PA and acting as a substrate for plasmin. The activation of plasminogen by t-PA is controlled by specific inhibitors, plasminogen activator inhibitors and α2-antiplasmin. Additional plasmin(ogen) binding sites are created by degradation of fibrin during lysis, a positive feedback system accelerating fibrinolysis, since plasmin has binding specificity for the C-terminal lysine residues it generates by cleavage. Individual molecules of t-PA can activate many plasminogen molecules, also accelerating the rapid cleavage of fibers.

Thrombolytic therapy is used in the treatment of both arterial and venous thrombotic disease. High intensity ultrasound can be delivered via catheter or transcutaneously to mechanically disrupt clots. Low intensity ultrasound does not destroy clots directly but enhances lysis initiated by t-PA. The potential of low intensity ultrasound to enhance fibrinolysis for treatment of thrombotic diseases has been studied extensively. Studies in vitro have shown that the enhancement of lysis is non-thermal and involves increased transport of and binding of t-PA to fibrin, as well as changes in fibrin structure, including reversible disaggregation of fibrin fibers. The effects of ultrasound have been confirmed by in vivo animal studies showing increased reperfusion and minimal toxicity in both coronary and peripheral vessels.

Although the effects of ultrasound on fibrinolysis have been studied, this field has been hampered by lack of a simple and accurate method to follow the time course of digestion. Here we introduce such a method used elsewhere, monitoring of turbidity to follow lysis. t-PA is mixed with thrombin and the plasma is recalcified. Thrombin converts fibrinogen to fibrin to form the gel, and the ensuing fibrin acts as a co-factor to form the ternary complex of plasminogen-t-PA-fibrin, so that plasminogen is converted to plasmin, which digests fibrin in a process called internal lysis. There is a well-developed theory that turbidity is directly related to clot structure: turbidity is proportional to the average cross-sectional area of the fibers. Moreover, this turbidity measurement allows accurate monitoring of the kinetics of clot structural changes during ultrasound-enhanced fibrinolysis without disturbing the processes involved and provides good time resolution. In our studies, structural changes of platelet-poor plasma clots during fibrinolysis were visualized by deconvolution microscopy, and the dynamics were followed by fluorescence recovery after photobleaching. We report here the direct observation of the effects of ultrasound on fibrinolysis by coordinated studies using these methods and provide evidence of the mechanisms involved.

Methods

Ultrasound exposure chamber

To quantify ultrasound-accelerated lysis in fibrin clots and examine changes to individual fibers, an ultrasound exposure chamber was constructed on a microscope slide, using lead zirconate-titanate bars 0.5 × 2 × 25mm (PiezoKinetics, Bellefonte, PA), with poling and electrode placement so that they could deform in a thickness-mode resonance at 760kHz across the 2mm dimension. Two such bars were glued to a microscope slide in a parallel configuration, with 12mm spacing between them (Fig. 1A). A cover slip was affixed across the bars with silicone vacuum grease, creating a 0.5mm-depth chamber for clot formation, and the two remaining sides of this chamber were sealed. The bars had the two innermost faces electrically grounded; the outer faces were connected electrically to a 50W power amplifier (Amplifier Research 50A15, Souderton, PA) driven by a function generator (Agilent 33120A, Englewood, CO). Thus, when the crystals were activated with pulses of 760 acoustic periods each, for a pulse duration of 1ms, planar acoustic standing waves were set up in the clot across the slide.

Calibration of the ultrasonic pressure amplitude was accomplished using a 0.2mm-diameter polyvinylidene difluoride needle hydrophone (Precision Acoustics, Dorchester UK) inserted into the space between cover slip and microscope slide. When a sinusoidal voltage of 30V peak-to-peak was applied to the crystals, an ultrasonic standing wave was launched in the medium, as verified by the presence of alternating pressure nodes and antinodes across the clot between the crystals (Fig. 1B), with maximum pressure amplitude in a plane midway between the two crystals.

Sample Preparation and Ultrasound Exposure

Platelet-poor plasma clots were prepared by mixing 26mM $CaCl_2$ with 1.5 μl of 50 U/ml thrombin in 50mM Tris-HCl, 140mM NaCl for a final concentration of 0.5U/ml thrombin and 150μl of pooled plasma from six healthy volunteers following approval by the Institutional Review Board and informed consent of the donors. Polymerization of purified fibrinogen was carried out by mixing of purified human plasminogen-free fibrinogen (Hyphen BioMed, France) at a final concentration of 1.5 mg/ml in 50 mM Tris-HCl, 140 mM NaCl, pH 7.4, 3 mM $CaCl_2$ with 0.5U/ml final concentration of thrombin. Single-chain recombinant t-PA (American Diagnostica, Greenwich, CT) was added to the plasma mixture to a final concentration of 2.9μg/ml, which is in the clinical range of maximum lytic effect. After polymerization, plasma clots were exposed to 760kHz ultrasound: 760 acoustic cycles per tone burst (e.g., 1ms duration) with pulse-repetition frequencies (PRFs) of 20, 50, and 80Hz. All acoustic pressure amplitudes were maintained on the centerline (0.7MPa peak-to-peak) (Fig. 1B).

For a second type of experiment, fibrin was polymerized as described above, but no t-PA was added. After the turbidity reached a plateau, clots were exposed to ultrasound with 1ms-duration tone bursts at 50Hz PRF and 0.7MPa peak-to-peak amplitude.

Turbidity measurements

Polymerization and internal lysis were followed by monitoring of changes in turbidity as a function of time at 37°C, as determined by thermocouple measurement and infrared thermometry. Turbidity measurements were carried out at a wavelength of 350nm using a DU640 spectrophotometer (Beckman Coulter, Fullerton, CA), with a beam width of 1.8mm, aligned through the clot midway between the two crystals. The lysis time was defined as twice the time from maximum turbidity to ½ the maximum, which avoids problems of unusual turbidities as the baseline is approached.

Temperature measurements

The temperature of the clot was measured during exposure to ultrasound with a 50μm-diameter K-type thermocouple wire mounted inside the clot at the midpoint between the two crystals. An infrared thermometer was also used; its region of sensitivity encompassed nearly the entire clot (Omega OSXL689, Stamford, CT). The microscope slide was then placed in temperature-controlled 37°C surroundings throughout subsequent exposures.

Deconvolution Light Microscopy

To monitor morphological changes during lysis of clots, Alexa 488 labeled fibrinogen was added to the polymerization mixture as a tracer: 0.05mg/ml final concentration of Alexa 488 labeled fibrinogen (Invitrogen, Carlsbad, CA 92009) with a degree of labeling of 6 molecules of dye per molecule of protein. Images were taken every 10min until the clot was completely lysed using a DeltaVision Spectris Restoration microscopy system equipped with Olympus IX–70 inverted microscope with a 10X objective lens. Epi-fluorescence illumination was provided by a HBO-100W mercury arc lamp, and the excitation wavelength of 470nm was selected with an electronic filter wheel containing a filter for Alexa 488, dichromatic mirror and emission filter of 520nm. SoftWorx software, part of DeltaVision Spectris Restoration microscopy system, was used for image processing, including deconvolution based on a Constrained-Iterative Method. At least three deconvolution microscopy experiments were carried out to allow quantitative analysis.

Fluorescence recovery after photobleaching during exposure of fibrin clots to ultrasound

Fluorescence Recovery After Photobleaching (FRAP) was used to characterize the mobile fraction of fibrin in clots during exposure to ultrasound. FRAP experiments were carried out with a Zeiss 510 LSM confocal microscope, using the LSM acquisition software (Carl Zeiss, Thornwood, NY), equipped with a 20X objective lens, and an argon ion 488nm laser. The gain and offset of the detector are the most critical parameters to set up before collecting FRAP images. The offset was set to see background pixels slightly higher than zero to catch all possible changes in the sample signal. The detector gain was set to a level such that very few or no pixels were saturated. Areas of 24.3X146.3μm were photobleached with 100% output of the 488nm laser for 20 μsec/pixel. Five pre-bleached images were collected, and those images were used as a reference for the steady-state distribution of the fluorescent molecules for FRAP analyses. Images of fluorescence recovery were collected at 2% of excitation laser power.

The binding reaction that occurs in our FRAP experiments is:

$$F+S \leftrightarrow C, \quad (1)$$

where F represents the free fibrin monomers, S represents the vacant binding sites on immobile fibers, and C (which is FS) represents the bound complex. k_{on} and k_{off} are the on and off rates for the forward and backward reactions respectively. We assume that this reaction is at equilibrium before photo-bleaching in the FRAP experiment. This implies that the concentrations of F, S and C have reached their constant equilibrium values F_{eq}, S_{eq} and C_{eq} by the time FRAP is performed. We also assumed that no movement of fibrin molecules occurred during photobleaching and minimal photobleaching occurs during the recovery phase and that diffusion is very fast. In such a scenario, the rate at which the number of bound complexes evolves is given by,

$$\frac{d[C]}{dt} = k_{on} S_{eq} F_{eq} - k_{off}[C], \quad (2)$$

The solution to this equation is:

$$[C](t) = C_{eq}(1 - \exp(-k_{off} t)), \quad (3)$$

where $C_{eq} = k_{on} S_{eq} F_{eq} / k_{off}$ is the equilibrium concentration of C, and we have assumed the initial condition that at $t = 0$, $[C](0) = 0$. We fit the FRAP recovery curves using this formula and obtained the values of the off-rate k_{off} and C_{eq} assuming that the contribution of F_{eq} to the fluorescence is very small. The least squares method was used for the fitting.

Image Analysis

Metamorph software (Molecular Devices, Sunnyvale, CA) was used for image analysis. To investigate progressive changes in the fibrin network as a function of time, the network images were thresholded manually and total fluorescence of fibers was measured for each time point.

For each FRAP experiment, fluorescence intensity measurements were performed by measuring the fiber network intensity and the intensity in all areas between fibers by using Metamorph. The raw intensity measurements were imported into Excel (Microsoft, Redmond, WA) for further analyses. Those data were fitted by using eqn. (3) above.

Results

The use of turbidity to follow the effects of ultrasound on internal lysis

Turbidity measurements, used to evaluate the effects of ultrasound on internal lysis in plasma clots initiated by t-PA, showed that rate of lysis was enhanced considerably (Fig. 2). Exposure to 1ms-duration tone bursts of 760kHz ultrasound and a 50Hz pulse repetition rate

lysed clots 2.3× faster than those that were not exposed to ultrasound ($p<0.001$ by a one-tailed t-test).

We investigated the effect of changing the pulse repetition frequency (PRF) on clot lysis (Fig. 2) using the same concentration of t-PA in all clots and the same tone burst duration and amplitude (1 ms and 0.7MPa p-p). In addition to the 50Hz pulse repetition rate, 20 and 80Hz PRF were employed and turbidity plotted as a function of time for 10 successive experiments in each condition. The lysis times were: control, 139 min; 50Hz, 60.5 min; 20Hz, 98 min; 80 Hz, 86.1 min. Thus, changing the PRF to 20 and 80Hz reduced lysis time 1.4× and 1.6x, respectively compared to controls ($p < 0.001$ by one-tailed t-test) (Fig. 2). However, increasing the PRF to 80Hz did not produce a greater effect on fibrinolysis than 50Hz, 1.6× compared to 2.3×.

Effect of ultrasound on plasma clots in the absence of t-PA

As a control, to ensure that the effects of ultrasound were a consequence of modulation of the activity or binding of t-PA and/or plasmin(ogen), and not some other unknown effects, we exposed plasma clots containing no t-PA to ultrasound using the setting for which a maximum fibrinolytic effect had been produced: 760kHz, 1ms-duration, 50Hz PRF. We found that no lysis occurred, but observed an interesting minor effect on the time-course of turbidity (Fig. 3). There was a slight decrease in turbidity of clots exposed to ultrasound compared to no-ultrasound controls ($p < 0.01$). This decrease was reproduced reliably ($p < 0.01$ by single-tailed t-test) in each of 10 trials. To exclude the possibility that this decrease in turbidity arose from ultrasound enhancement of lysis by contaminants of t-PA in the plasma, we also did experiments with clots made from purified, plasminogen-free fibrinogen with added 0.5U/ml thrombin (Fig. 3). The results were very similar to those from the plasma experiments, demonstrating that no lysis was occurring.

Effect of ultrasound on the temperature of clots

Ultrasound caused elevation in temperature of the plasma clots of only a maximum of 0.8°C over 3hr of exposure, as measured by a thermocouple and by infrared thermometry. This temperature change by itself would be expected to have negligible effects on clot lysis rates.

Imaging of fibrinolysis of plasma clots exposed to ultrasound

Direct observation of plasma clots undergoing internal lysis with and without ultrasound exposure as a function of time was performed using deconvolution microscopy. Images of clots that were not exposed to ultrasound show that fibers degraded gradually and the fibrin network remained intact until it dissolved completely (Fig. 4A–D). On the other hand, imaging of clots exposed to ultrasound show that at the beginning of fibrinolysis, the fibrin network degraded gradually, similarly to those that were not exposed to ultrasound, (Fig. 4E,F), but when approximately 30% of the fibrin fibers disappeared, the clot broke into pieces and dissolved (Fig. 4G,H). Although we searched the microscope images for the micron-sized bubbles that would be expected from cavitation, i.e. those that would be resonant at about 1MHz, no such bubbles were observed. If such cavitation bubbles were present, they would be evident in the confocal images as black circular voids on the

background of fluorescence from the labeled fibrin(ogen), because they would exclude the labeled molecules that are inevitably remaining in solution.

The total fluorescence intensity of the fibrin network was measured and plotted as a function of time. Fitting analyses of those curves showed that the rate of lysis for the beginning of the process was similar for both experiments with and without ultrasound, with a rate of 0.13OD/min. However, the lysis rate changed after approximately 30% of the fibrin network disappeared for both experiments, with rates of 12.70OD/min with ultrasound and 0.55OD/min without ultrasound (Fig. 5).

Effect of ultrasound on the dynamics of fibrin related structures

Fluorescence Recovery After Photobleaching (FRAP) was used to characterize the mobile fraction of fibrin in clots during exposure to ultrasound. For these experiments, large areas 24X146μm, were photobleached and changes in fluorescence of the fibrin network due to ultrasound exposure after photobleaching were monitored as a function of time. Recovery curves show the rate and extent of recovery (Fig. 6).

If we fit the FRAP recovery curves for the control experiments using eqn. (3) (see Methods section), we get the off-rate for fibrin monomers dissociating from fibrin polymer $k_{off} = 0.0635 s^{-1}$ (std. dev. = $0.00217 s^{-1}$, n=3) and the equilibrium concentration of bound fibrin polymer complex C_{eq} = 1.89 (std. dev. = 0.26, n=3). Similarly, for the ultrasound experiments we get $k_{off} = 0.0894 s^{-1}$ (std. dev. = $0.0088 s^{-1}$, n=3) and C_{eq} = 2.76 (std. dev. = 0.19, n=3). The fitted values of k_{off} and C_{eq} are shown in Fig. 6D. Ultrasound increases the off-rate and the concentration of bound complex but the difference between the two off-rates is within one standard deviation. Since the maximum value of $C(t)$ is C_{eq} and this value is reached as $t \rightarrow \infty$ we plotted the fraction of recovery $rec(t) = C(t)/C_{eq}$ for both control and ultrasound. The trends looked very similar (Fig. 6A) and could be fitted with eqn. (3) with $k_{off} = 0.0721 s^{-1}$. We then used this k_{off} to determine C_{eq} for both control and ultrasound. This time we found that C_{eq} = 1.8987 for control and C_{eq} = 2.5025 for ultrasound (Fig. 6B, C). This result is consistent with earlier work, which suggests that ultrasound creates more binding/unbinding sites on the fibrin fibers (increased S_{eq}) and increases the interaction between the fibers and the free floating oligomers (better mixing).

Discussion

Effects of low and high frequency ultrasound on fibrinolysis have been studied for some time, but there has not been a convenient method to precisely monitor the time course of lysis. Many studies have involved weighing clots as a function of time to measure mass loss or using radioactively-labeled fibrin. We have developed a unique ultrasound exposure chamber that makes it simple and easy to monitor lysis quantitatively over time and can be used for both measuring turbidity and imaging changes in the fibrin network.

Our results indicate that the effect of ultrasound on lysis is not thermal, in contrast to one previous study that showed an increase in the temperature of plasma clots under other conditions, with more intense 1–3.5MHz ultrasound, at an acoustic intensity of $2 W/cm^2$. The results of this study showed that raising the temperature in a clot by 6°C may increase

the lysis rate approximately 2x. However, many other studies with lower intensity ultrasound have also found that lysis can be enhanced with no thermal effects.

The mechanism of low intensity ultrasound accelerated thrombolysis has been unclear. Cavitation itself can enhance fibrinolysis. Some studies have shown that cavitation can be reduced by application of static pressure. However, in these experiments only about half the acceleration of fibrinolysis due to ultrasound could be removed by static pressure, suggesting that there is another major mechanism in addition to cavitation. Studies showing that uptake of t-PA into clots is increased by ultrasound as well as binding of t-PA to fibrin support this suggestion.

The ultrasound system used for these experiments was designed to minimize cavitation, so that this was not a significant mechanism of the enhancement of lysis. We found that there were differences in the dynamics of fibrin network disappearance as a result of ultrasound. At the beginning of both the turbidity curves and the measurements of fluorescence loss in the micrographs, the rate of lysis was about the same with and without ultrasound. After about 30% of the fibrin network was degraded, the rate of fibrinolysis increased substantially more with ultrasound than without (Fig. 2,4G). The first part of the process, represented by the beginning slope of turbidity curves and initial rate of loss of fluorescence in microscopy images, does not appear to be much affected by ultrasound. Although the binding of t-PA to fibrin is enhanced by ultrasound, the primary effect of the ultrasound appears to occur later. It could be that the first part of both of these curves is determined primarily by k_{off} of the unbinding reaction, which is not much affected by ultrasound. Later steps of lysis, as represented in both the slope of the second phase of the turbidity and fluorescence loss, are greatly accelerated by ultrasound, further discussed below.

There was not a linear relationship between the PRF and the lysis rate. These results suggest that there may be a resonance frequency related to fibrin protofibril or fiber lengths in the clots, such that certain frequencies have greater effects than others.

Deconvolution microscopy allows direct visualization of the changes to clot structure over time through removal of out-of-focus light. While the normal process of fibrinolysis involves gradual digestion of the network, in the presence of ultrasound the network disappears precipitously. This observation was quantified by measurement of the total fluorescence as a function of time (Fig. 5). Like the turbidity curves, there is an initial slope that is similar with and without ultrasound and then the slope of the second part of the fluorescence decrease is much more rapid with ultrasound. However, the curves from turbidity and fluorescence are not identical, but the difference between them can be interpreted together with all the other results presented here. With ultrasound, the turbidity decreases sooner than the total mass (fluorescence). Previous studies have shown that ultrasound causes reversible disaggregation of fibrin, resulting in thinner fibers, consistent with lower turbidity. Then, the total mass decreases precipitously. Without ultrasound, the turbidity decreases slower while the total mass decreases faster. During lysis fibers are cut laterally, which would be consistent with not much change in fiber diameter initially, but there would be some decrease in mass from the lysis in the vicinity of that first t-PA initiation site.

Moreover, by following the effects of ultrasound without any enzymatic action through turbidity measurements, we observed a slight effect of ultrasound by itself (Fig. 3), which likely corresponds to a change in clot structure, a decrease of the fiber diameter, because the turbidity is proportional to the average cross-sectional area of the fibers. Moreover, a decrease of fiber diameter is in agreement with results showing by scanning electron microscopy that ultrasound can cause disaggregation of fibrin into thinner fibers.

These results of the effects of ultrasound on fibrin structure with and without lysis can be accounted for by a recent study demonstrating that fibrin is an equilibrium polymer. In other words, there is turnover in a fibrin clot, such that monomers or oligomers can dissociate and re-associate, primarily from the surface of fibers. Also, the equilibrium can be shifted toward dissociation under certain conditions, for example perfusion of the GPRP peptide, which mimics the knob 'A' that competes with fibrin for holes 'a'. Ultrasound causes a similar shift toward dissociation and consequently a decrease in the diameter of the fibers, probably because of increased tension in the fibers from vibration, while the total volume of the fibers remains fixed. This results in an increase in the surface area of the fibers, so that there are more binding/unbinding sites for t-PA/plasmin(ogen). This is consistent with FRAP results that show ultrasound causes an increase in the equilibrium concentration of vacant binding sites on fibrin polymer, S_{eq}.

Analysis of FRAP data of digesting clots shows that values of the off-rate for fibrin monomers dissociating from fibrin polymer, k_{off}, are unaffected by ultrasound while the equilibrium concentration of bound fibrin polymer complex, $C_{eq,}$ is higher with ultrasound, meaning that there is an increase in binding/unbinding sites. It could also be that C_{eq} is higher because of the increased mixing and transport from ultrasound. During fibrinolysis, there is a positive feedback system that accelerates the process by creation of additional plasmin(ogen) binding sites from the degradation of fibrin and creation of more C-terminal lysines, since plasmin cleaves at lysine residues. However, our results suggest that ultrasound has a dramatic effect on the creation of additional binding sites, probably through changes in structure discussed above. In fact, there could be second positive feedback loop that is active here, such that vibration causes an increase in tension in the fibers, which results in a quicker decrease in the fiber diameter due to accelerated lysis. As a result, the stress in the fibers rapidly increases and causes its collapse. This finding is in agreement with the result here that ultrasound by itself promotes dissociation of fibrin monomers or oligomers leading to decreased fiber diameter and hence lower clot turbidity.

Thus, we can explain the dramatic increase of fibrinolysis by ultrasound. Ultrasound by itself promotes disaggregation of fibrin structures, which results in increase of binding sites for t-PA and plasmin(ogen), so that cleavage occurs at more locations.

Conclusions

In this study, turbidity measurements, deconvolution microscopy, and fluorescence recovery after photobleaching were used to investigate fibrinolysis in the presence of ultrasound dynamically with excellent time and image resolution. Turbidity experiments without t-PA show that ultrasound causes a decrease in the diameter of the fibers, which means an increase in the surface area of the fibers, so more plasmin(ogen)/t-PA binding/unbinding

sites become available. The likely mechanism of this structural change is the increase of tension in the protofibrils as a result of vibration, which results in a quicker disintegration and decrease in the fiber diameter. In addition, there is increased mixing and transport of t-PA/plasmin(ogen) resulting from ultrasound. The positive feedback of these combined mechanisms accounts for the very striking effects of ultrasound on fibrinolysis. Although the experiments here were designed to investigate and understand basic mechanisms of fibrinolysis, the findings have significance for improving methods of clinical thrombolysis.

Acknowledgments

We acknowledge the support of NIH grant HL090774. PKP acknowledges partial support from NSF through grant number NSF CMMI 1066787.

References

1. Weisel JW, Litvinov RI. The biochemical and physical process of fibrinolysis and effects of clot structure and stability on the lysis rate. Cardiovasc & Hematol Agents Med Chem. 2008; 6:161–80. [PubMed: 18673231]
2. Stone MJ, Frenkel V, Dromi S, Thomas P, Lewis RP, Li KC, Horne M 3rd, Wood BJ. Pulsed-high intensity focused ultrasound enhanced tPA mediated thrombolysis in a novel in vivo clot model, a pilot study. Thromb Res. 2007; 121:193–202. [PubMed: 17481699]
3. Weiss HL, Selvaraj P, Okita K, Matsumoto Y, Voie A, Hoelscher T, Szeri AJ. Mechanical clot damage from cavitation during sonothrombolysis. J Acoustical Soc Amer. 2013; 133:3159–75.
4. Soltani A, Soliday C. Effect of ultrasound on enzymatic activity of selected plasminogen activators. Thromb Res. 2007; 119:223–8. [PubMed: 16545433]
5. Blinc A, Francis CW, Trudnowski JL, Carstensen EL. Characterization of ultrasound-potentiated fibrinolysis in vitro. Blood. 1993; 81:2636–43. [PubMed: 8490172]
6. Siegel RJ, Suchkova VN, Miyamoto T, Luo H, Baggs RB, Neuman Y, Horzewski M, Suorsa V, Kobal S, Thompson T, Echt D, Francis CW. Ultrasound energy improves myocardial perfusion in the presence of coronary occlusion. J Amer Coll Cardiol. 2004; 44:1454–8. [PubMed: 15464327]
7. Ferri F, Greco M, Arcovito G, Bassi FA, De Spirito M, Paganini E, Rocco M. Growth kinetics and structure of fibrin gels. Phys Rev E Stat Nonlin Soft Matter Phys. 2001; 63:031401. [PubMed: 11308648]
8. Pieters M, Hekkenberg RT, Barrett-Bergshoeff M, Rijken DC. The effect of 40 kHz ultrasound on tissue plasminogen activator-induced clot lysis in three in vitro models. Ultrasound Med & Biol. 2004; 30:1545–52. [PubMed: 15588966]
9. Siddiqi F, Odrljin TM, Fay PJ, Cox C, Francis CW. Binding of tissue-plasminogen activator to fibrin: effect of ultrasound. Blood. 1998; 91:2019–25. [PubMed: 9490686]
10. Francis CW, Suchkova VN. Ultrasound and thrombolysis. Vasc Med. 2001; 6:181–7. [PubMed: 11789973]
11. Sakharov DV, Barrertt-Bergshoeff M, Hekkenberg RT, Rijken DC. Fibrin-specificity of a plasminogen activator affects the efficiency of fibrinolysis and responsiveness to ultrasound: comparison of nine plasminogen activators in vitro. Thromb Haemost. 1999; 81:605–12. [PubMed: 10235448]
12. Francis CW, Blinc A, Lee S, Cox C. Ultrasound Accelerates Transport of Recombinant Tissue-Plasminogen Activator into Clots. Ultrasound Med & Biol. 1995; 21:419–24. [PubMed: 7645133]
13. Kashyap A, Blinc A, Marder VJ, Penney DP, Francis CW. Acceleration of fibrinolysis by ultrasound in a rabbit ear model of small vessel injury. Thromb Res. 1994; 76:475–85. [PubMed: 7900095]
14. Alexandrov AV. Ultrasound enhancement of fibrinolysis. Stroke. 2009; 40:S107–10. [PubMed: 19064806]

15. Alonso A, Della Martina A, Stroick M, Fatar M, Griebe M, Pochon S, Schneider M, Hennerici M, Allemann E, Meairs S. Molecular imaging of human thrombus with novel abciximab immunobubbles and ultrasound. Stroke. 2007; 38:1508–14. [PubMed: 17379828]
16. Carr ME Jr, Hermans J. Size and density of fibrin fibers from turbidity. Macromol. 1978; 11:46–50.
17. Francis CW. Ultrasound-enhanced thrombolysis. Echocardiography. 2001; 18:239–46. [PubMed: 11322907]
18. Agard DA. Optical sectioning microscopy: cellular architecture in three dimensions. Annual Rev Biophys Bioeng. 1984; 13:191–219. [PubMed: 6742801]
19. Chernysh IN, Nagaswami C, Purohit PK, Weisel JW. Fibrin clots are equilibrium polymers that can be remodeled without proteolytic digestion. Sci Rep. 2012; 2:879. [PubMed: 23170200]
20. Lauer CG, Burge R, Tang DB, Bass BG, Gomez ER, Alving BM. Effect of ultrasound on tissue-type plasminogen activator-induced thrombolysis. Circulation. 1992; 86:1257–64. [PubMed: 1394932]
21. Sakharov DV, Hekkenberg RT, Rijken DC. Acceleration of fibrinolysis by high-frequency ultrasound: the contribution of acoustic streaming and temperature rise. Thromb Res. 2000; 100:333–40. [PubMed: 11113277]
22. Sapozhnikov OA, Khokhlova VA, Bailey MR, Williams JC Jr, McAteer JA, Cleveland RO, Crum LA. Effect of overpressure and pulse repetition frequency on cavitation in shock wave lithotripsy. J Acoust Soc Amer. 2002; 112:1183–95. [PubMed: 12243163]
23. Suchkova V, Siddiqi FN, Carstensen EL, Dalecki D, Child S, Francis CW. Enhancement of fibrinolysis with 40-kHz ultrasound. Circulation. 1998; 98:1030–5. [PubMed: 9737524]
24. Francis CW, Onundarson PT, Carstensen EL, Blinc A, Meltzer RS, Schwarz K, Marder VJ. Enhancement of fibrinolysis in vitro by ultrasound. J Clin Invest. 1992; 90:2063–8. [PubMed: 1430229]
25. Nahirnyak VM, Yoon SW, Holland CK. Acousto-mechanical and thermal properties of clotted blood. J Acoust Soc Amer. 2006; 119:3766–72. [PubMed: 16838520]
26. Datta S, Coussios CC, McAdory LE, Tan J, Porter T, De Courten-Myers G, Holland CK. Correlation of cavitation with ultrasound enhancement of thrombolysis. Ultrasound Med & Biol. 2006; 32:1257–67. [PubMed: 16875959]
27. Miller DL. Particle gathering and microstreaming near ultrasonically activated gas-filled micropores. J Acoust Soc Amer. 1988; 84:1378–87. [PubMed: 3198872]
28. Kondo T, Kodaira T, Kano E. Free radical formation induced by ultrasound and its effects on strand breaks in DNA of cultured FM3A cells. Free Radical Res Comm. 1993; 19(Suppl 1):S193–200.
29. Prokop AF, Soltani A, Roy RA. Cavitational mechanisms in ultrasound-accelerated fibrinolysis. Ultrasound Med & Biol. 2007; 33:924–33. [PubMed: 17434661]
30. Chuang YH, Cheng PW, Chen SC, Ruan JL, Li PC. Effects of ultrasound-induced inertial cavitation on enzymatic thrombolysis. Ultrasonic Imaging. 2010; 32:81–90. [PubMed: 20687276]
31. Delius M, Ueberle F, Eisenmenger W. Extracorporeal shock waves act by shock wave-gas bubble interaction. Ultrasound Med & Biol. 1998; 24:1055–9. [PubMed: 9809639]
32. Everbach ECFC. Cavitational mechanisms in ultrasound-accelerated thrombolysis at 1 MHz. Ultrasound Med & Biol. 2000:1153–60. [PubMed: 11053750]
33. Soltani A, Volz KR, Hansmann DR. Effect of modulated ultrasound parameters on ultrasound-induced thrombolysis. Physics in Med and Biol. 2008; 53:6837–47.
34. Devcic-Kuhar B. Ultrasound affects distribution of plasminogen and tissue-type plasminogen activator in whole blood clots in vitro. Thromb Haemost. 2004; 92:980–5. [PubMed: 15543323]
35. Siddiqi F, Blinc A, Braaten J, Francis CW. Ultrasound increases flow through fibrin gels. Thromb Haemost. 1995; 73:495–8. [PubMed: 7667834]
36. Veklich Y, Francis CW, White J, Weisel JW. Structural studies of fibrinolysis by electron microscopy. Blood. 1998; 92:4721–9. [PubMed: 9845538]
37. Braaten JV, Goss RA, Francis CW. Ultrasound reversibly disaggregates fibrin fibers. Thromb Haemost. 1997; 78:1063–8. [PubMed: 9308755]

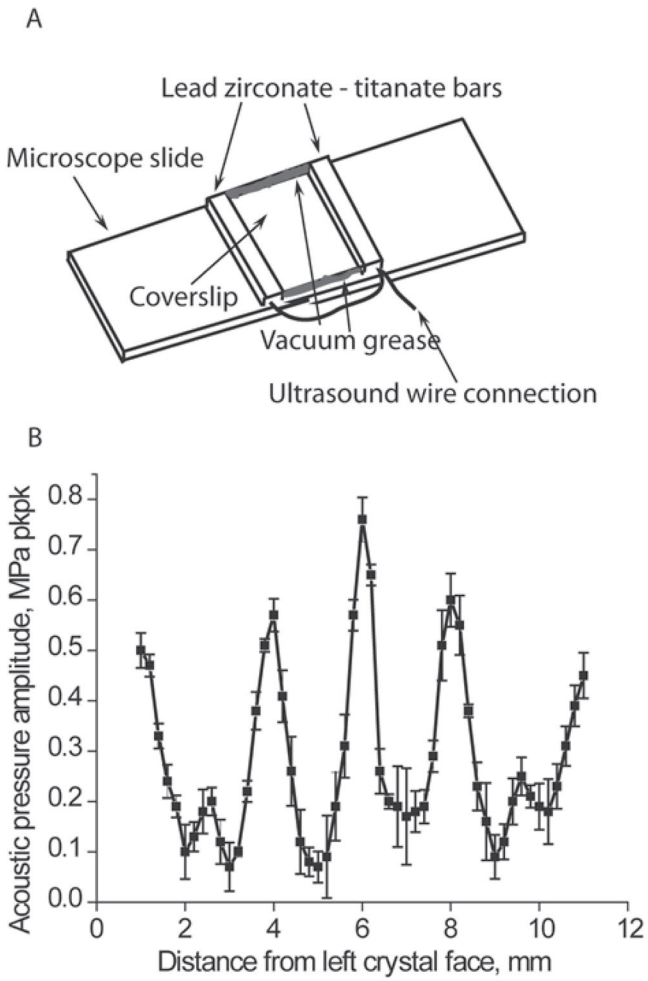

Fig. 1. Diagram of chamber and acoustic pressure measured across a chamber

(A) Diagram of chamber formed on a microscope slide between two lead-zirconate-titanate crystals. (B) Acoustic pressure amplitude measured across midsection of microscope slide between the crystals using a polyvinylidene difluoride needle hydrophone. Error bars are one standard deviation (n=10).

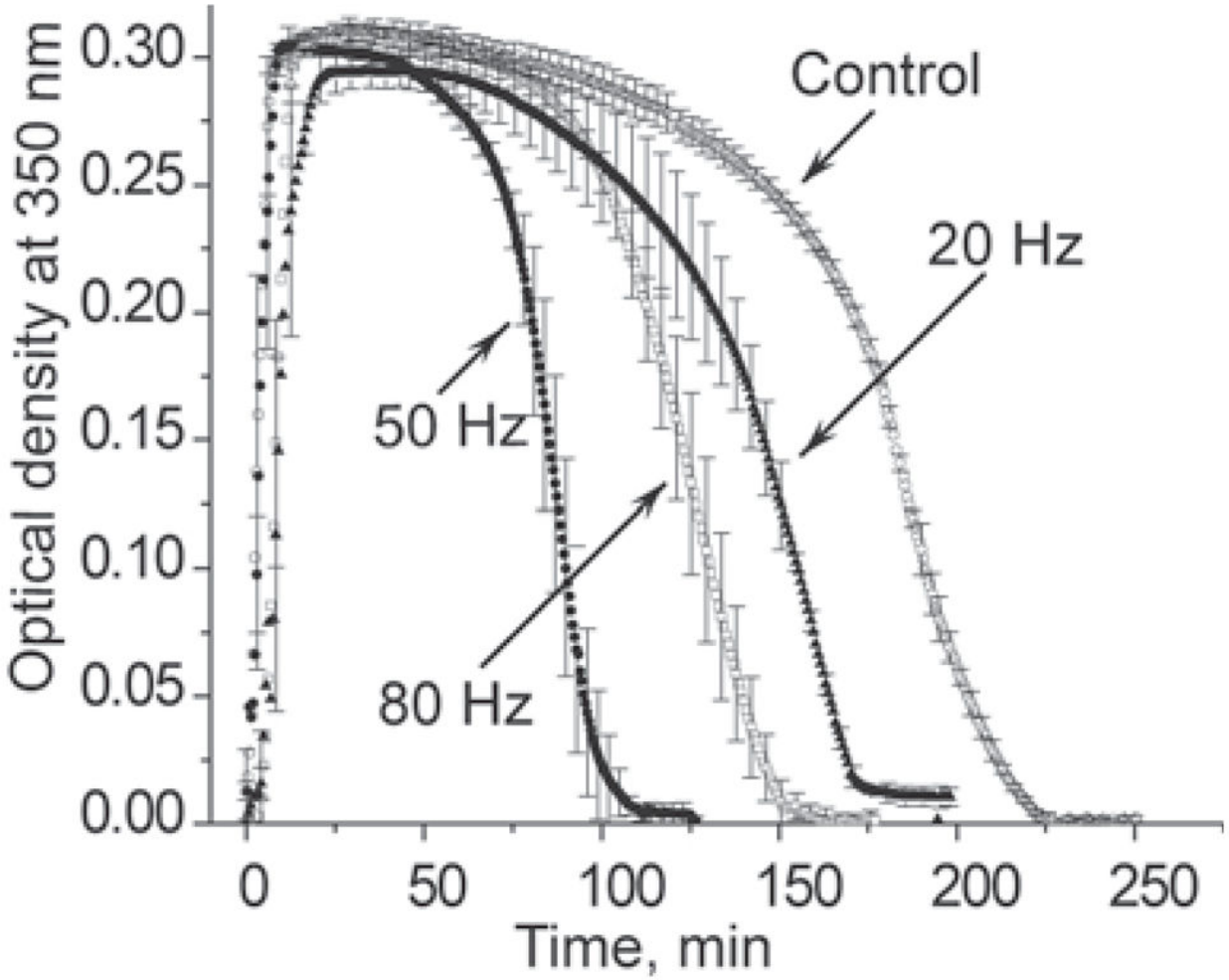

Fig. 2. Fibrinolysis of plasma clots as monitored by turbidity as a function of time

Control and effects of ultrasound on lysis with a fixed concentration of t-PA, with pulse-repetition frequencies (□) 80Hz; (●) 50Hz; (▲) 20Hz and (⌂) no ultrasound was applied. Curves represent means and standard deviations of 10 separate turbidity measurements as the change of optical density of a clot for each condition, plotted as a function of time

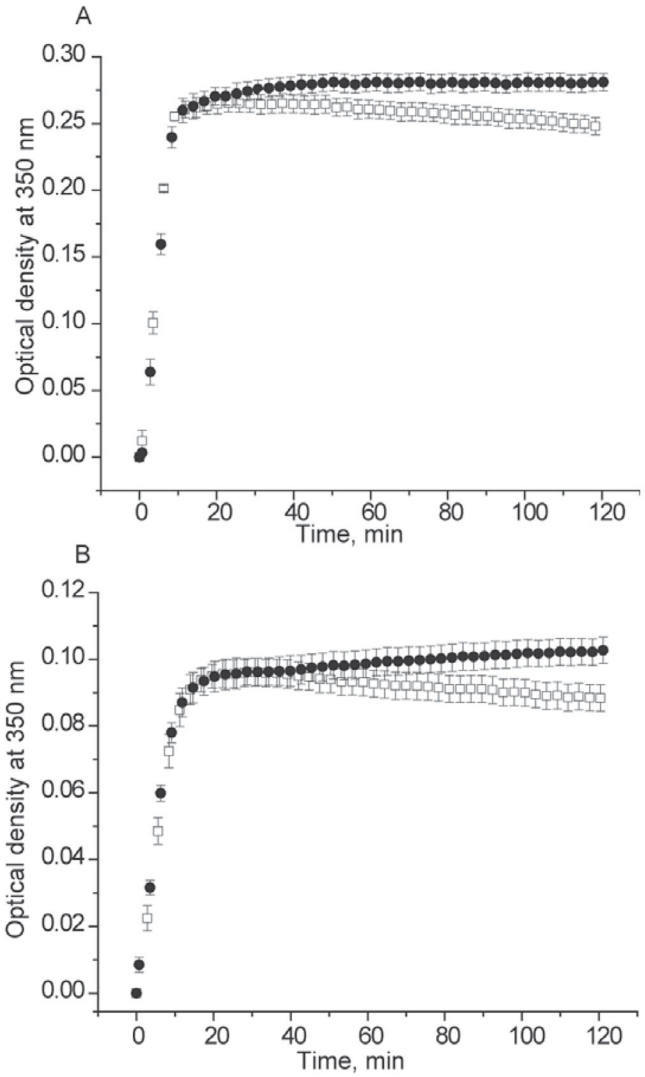

Fig. 3. Effect of ultrasound on the turbidity of plasma and fibrin clots without adding t-PA

760kHz ultrasound, 1ms-duration, pulse-repetition frequency of 50Hz. Clots were made from plasma with addition of 0.5U/ml thrombin (A) or from 1.5 mg/ml fibrinogen with 0.5IU/ml thrombin (B). Symbols represent (●) clot with no ultrasound; (□) clot with ultrasound.

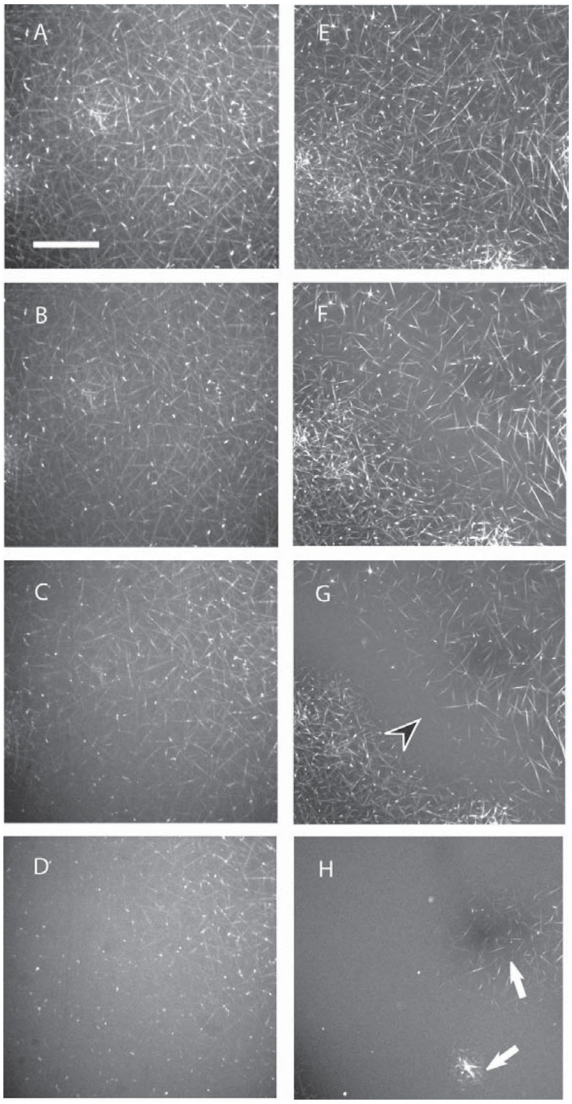

Fig. 4. Images obtained by deconvolution microscopy of plasma clots during fibrinolysis at different time points

(A, B, C, D) Images of lysis of plasma clots by t-PA with no ultrasound. (E, F, G, H) Images of lysis of plasma clots by t-PA and exposure to 50Hz ultrasound. Black arrowhead indicates discontinuity in the clot as a result of lysis in the presence of applied ultrasound. The white arrows indicate small portions of the network that are not yet lysed, while the rest of the clot network has been digested. Compare these images to the more continuous and gradual disappearance of the clot in the control sample without ultrasound. Bar = 20 μm.

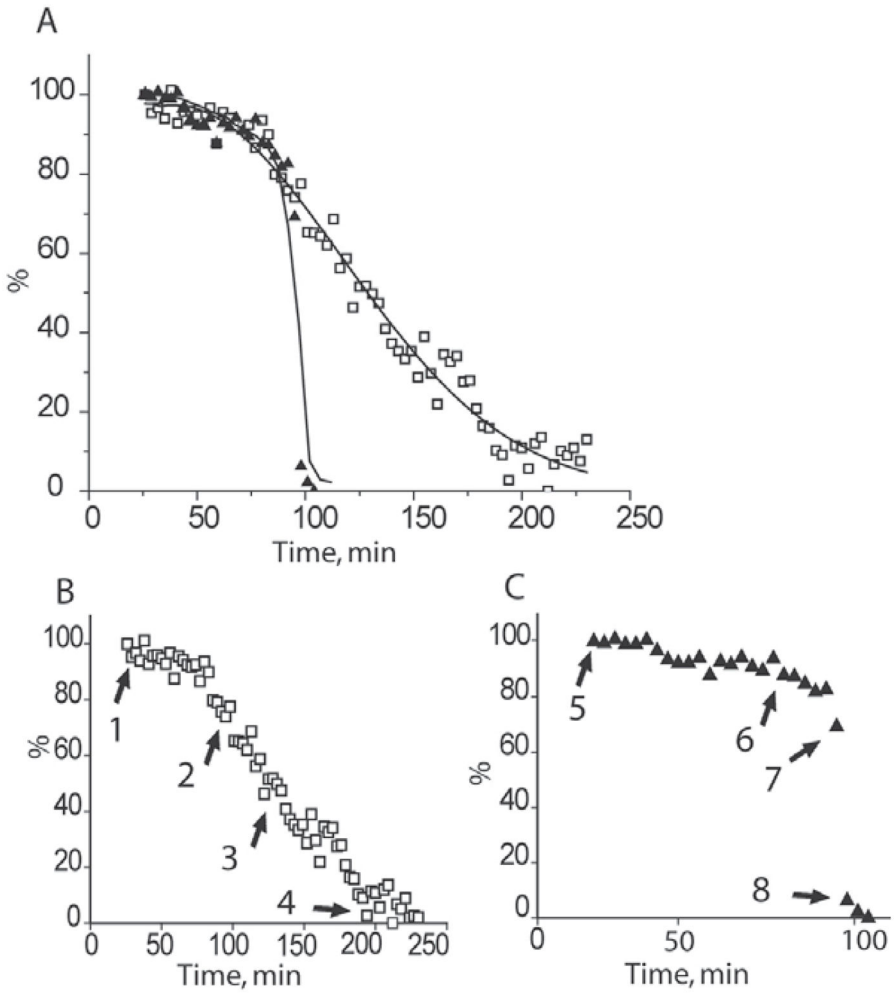

Fig. 5. Changes of fluorescence intensity of the microscope images from both clots with and without ultrasound as function of the time during fibrinolysis

(A) Superposition of both graphs of (□) fibrinolysis with t-PA but no ultrasound, (▲) fibrinolysis with t-PA and exposure to 50Hz ultrasound. The graphs are plotted on the same time scale for comparison. (B) fibrinolysis with t-PA but no ultrasound. Arrows 1, 2, 3, 4 indicate time points that correspond to images of Fig. 4 A, B, C, D, respectively. (C) fibrinolysis with t-PA and exposure to 50Hz ultrasound, plotted on a different time scale to visualize more details of the changes as a function of time. Arrows 5, 6, 7, 8 indicate time points that correspond to images Fig. 4 E, F, G, H, respectively.

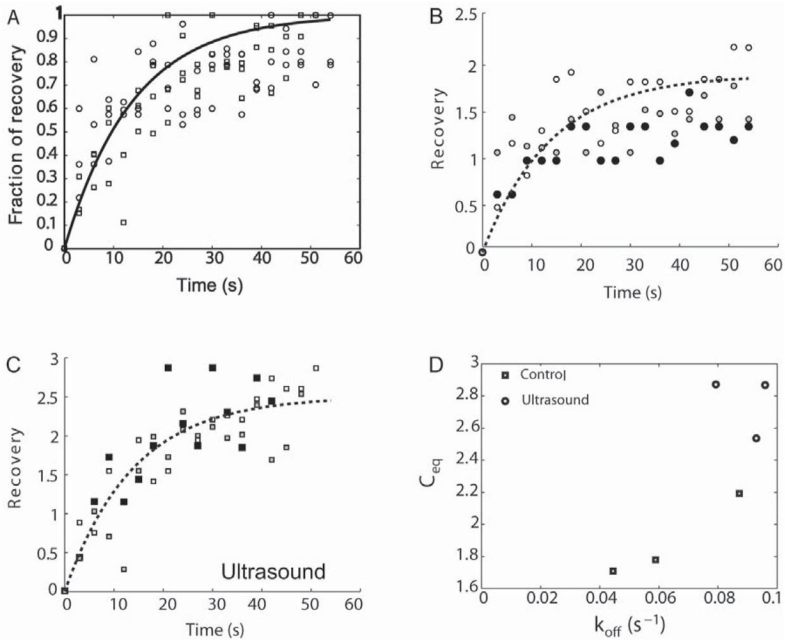

Fig. 6. Fluorescence recovery after photobleaching as a function of time

(A) Data points for both control and ultrasound experiments, three data sets each, fitting k_{off} = 0.0721 s–1. (B) Fitting of data without ultrasound, C_{eq} = 1.90. The dashed line again uses k_{off} = 0.0721 s–1. (C) Fitting of data with ultrasound. The dashed line also uses k_{off} = 0.0721 s–1 and fits C_{eq} = 2.50. This suggests that more binding sites become available when there is ultrasound. (D) If each set of FRAP data is fitted separately we extract the fitting parameters C_{eq} and k_{off}, which form a two-dimensional space in which each FRAP experiment represents a point. The points corresponding to control experiments have lower values of C_{eq} and k_{off} than those with ultrasound.